



The Temperature Effect on the Recombination Velocity at the junction Initiating the Short-Circuit Condition (SFCC) of a Silicon Solar Cell under External Electric Field

Marcel Sitor DIOUF¹, Ibrahima LY², Mamadou WADE², Ibrahima DIATTA¹, Youssou TRAORE¹, Mor NDIAYE¹, Grégoire SISSOKO¹

¹Laboratoire des Semi-conducteurs et d'Énergie Solaire, Faculté des Sciences et Techniques, Université Cheikh Anta Diop, Dakar, Sénégal

²Ecole Polytechnique de Thiès, Thiès, Sénégal

Abstract In this paper, we studied the influence of the electric field and temperature on the recombination velocity at the junction initiating the short-circuit and the short-circuit current. The excess of minority carrier's density in the base is determined from the continuity equation. The photocurrent and the short-circuit current are derived from the excess minority carrier's density. From the photocurrent study, the recombination velocity at the junction initiating the short-circuit and the short-circuit current are determined and studied for different values of electric field and the temperature under polychromatic illumination.

Keywords Temperature, Electric field, Recombination velocity, Short-Circuit Current

1. Introduction

The solar cell is a device that ensures the transformation of light energy into electrical energy. To obtain it, a set of chemical, mechanical and thermal treatments is necessary. Therefore, these treatments have more or less adverse effects on the performance of the final device [1]. These effects are characterized by, ohmic and recombination optical losses [2]. The quality of the solar cell is closely related to its electronic parameters [3] and electrical [4], various characterization techniques have been developed in order to improve the manufacturing steps of the solar cell. These techniques are based on the measurement of optical effects [3] or electric [4-6] of the imperfections contained in the solar cell maintained in static regime [7-8] and under dynamic regime (transient and frequency) [9-10]. The photovoltaic conversion depends also on the temperature. The electrical performances of a silicon solar cell are very sensitive to the temperature [11]. Thus, on the incident energy totality, approximately 13% is extracted as electrical energy. Much of this energy is dissipated as heat, this which leads under radiation, at a relatively high operating temperature if energy not converted into electrical is not drained. Much of this energy is dissipated as heat, this which leads under radiation, at a relatively high operating temperature if energy whom was not converted into electrical is not drained. Our contribution in this work is to study the effect of temperature on the recombination velocity at the junction initiating the short circuit and short circuit current of a solar cell under external electrical bias.

2. Theory

In our study, a n+pp+ solar cell type is considered [12]. It is illuminated by its front face under polychromatic illumination and it is under external polarization by applying a voltage. Therefore, we will study the external electric field effect resulting from the polarization and temperature on the behavior of minority carriers in the base volume. The structure of this solar cell is shown in Figure 1:



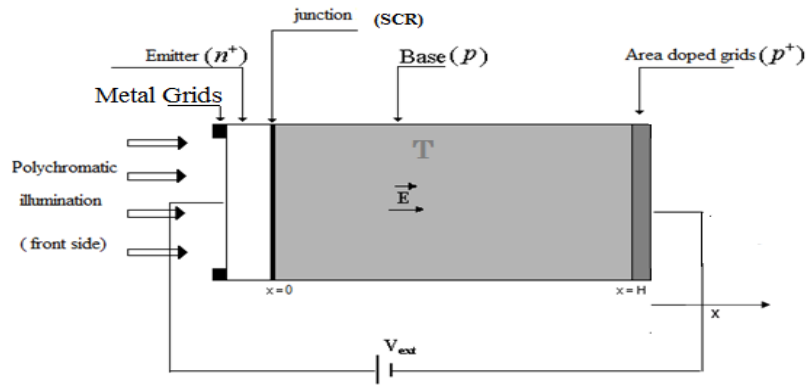


Figure 1: Solar cell structure to the $n^+ - pp^+$ type under electric polarization and polychromatic illumination.

2.1. Excess minority carrier’s density

The continuity equation for the excess minority carrier’s density photo-generated in the base under influence of the external electric field and temperature is:

$$\frac{\partial^2 \delta(x)}{\partial x^2} + \frac{\mu(T) \cdot E}{D(T)} \cdot \frac{\partial \delta(x)}{\partial x} - \frac{\delta(x)}{L(T)^2} + \frac{G(x)}{D(T)} = 0 \tag{1}$$

$\delta(x)$ is the excess minority carriers density according to the depth x in the base of the solar cell, $\mu(T)$ the electrons mobility coefficient and depends on the temperature [13]:

$$\mu(T) = 1,43 \cdot 10^9 \cdot T^{-2,42} \text{ cm}^2 \cdot \text{V}^{-1} \cdot \text{s}^{-1} \tag{2}$$

E represents the electric field, $D(T)$ the diffusion coefficient, $L(T)$ the diffusion length and are functions of the temperature:

$$D(T) = \mu(T) \cdot \frac{k_b}{q} \cdot T \tag{3}$$

$$L(T)^2 = \tau \cdot D(T) \tag{4}$$

k_b is the Boltzmann constant, q the charge of an electron and T is the temperature.

Posing in:

$$L_E(T) = \frac{\mu(T) \cdot E \cdot L(T)^2}{D(T)} \tag{5}$$

Equation (1) becomes:

$$\frac{\partial^2 \delta(x)}{\partial x^2} + \frac{L_E(T)}{L(T)^2} \cdot \frac{\partial \delta(x)}{\partial x} - \frac{\delta(x)}{L(T)^2} + \frac{G(x)}{D(T)} = 0 \tag{6}$$

$G(x)$ is the carrier generation rate of the minority carrier in the base [14] given by:

$$G(x) = \sum_{i=1}^3 a_i \cdot e^{-b_i \cdot x} \tag{7}$$

H is the thickness of the base.

The parameters a_i and b_i stem from the modeling of the incident illumination as defined by under A.M 1.5 condition [15]. These coefficients are given in Table 1:

Table 1 : values of the radiation coefficients defined under A.M 1.5

i	1	2	3
$a_i \text{ (cm}^{-3} \cdot \text{s}^{-1}\text{)}$	$6,13 \cdot 10^{20}$	$0,54 \cdot 10^{20}$	$0,0991 \cdot 10^{20}$
$b_i \text{ (cm}^{-1}\text{)}$	6630	1000	130

The excess of minority carrier’s density is obtained from equation (6) resolution and is given by:

$$\delta(x, T, E) = e^{\beta(T) \cdot x} \cdot [A \cdot ch(\phi(T) \cdot x) + B \cdot sh(\phi(T) \cdot x)] + \sum_{i=1}^3 c_i(T) \cdot e^{-b_i \cdot x} \tag{8}$$

With :

$$\phi(T) = \frac{(L_E^2(T) + 4 \cdot L^2(T))^{\frac{1}{2}}}{2 \cdot L^2(T)}, \quad \beta(T) = \frac{-L_E(T)}{2 \cdot L^2(T)}$$

$$c_i = -\frac{a_i \cdot L^2(T)}{D(T) \cdot [L^2(T) \cdot b_i^2 - L_E(T) \cdot b_i - 1]}$$

A and B are obtained with the boundary condition at the emitter – base junction and at the back surface of the cell [8, 14]:

-at the junction (x=0) :

$$\left. \frac{\partial \delta(x, T, E)}{\partial x} \right|_{x=0} = \frac{Sf}{D} \cdot \delta(0) \tag{9}$$

-at the back surface (x=H):

$$\left. \frac{\partial \delta(x, T, E)}{\partial x} \right|_{x=H} = -\frac{Sb}{D} \cdot \delta(H) \tag{10}$$

Sf and Sb are respectively excess minority carrier’s recombination velocities at the junction and at the back surface [14,16-17]. Sf characterizes the solar cell operation point. It also corresponds to the gradient of the minority carrier’s at the junction. Sb determines the losses by recombination at the rear face (back surface field BSF).

2.1.1. Study of diffusion lengths of the minority charge carriers $L_E(T)$ and $L(T)$

The diffusion length L(T) of minority charge carriers at the absence of electrical polarization is a function of the temperature. $L_E(T)$ is the diffusion length of the minority charge carriers in the presence of an external electric field. It depends on the temperature. The study of these two concepts will allow to show from a certain value of the electric field, the minority carrier diffusion photogenerated charge in the base becomes very sensitive to temperature. Thus we respectively represent in Figures 2a and b the profiles of the diffusion lengths of minority carriers profiles of load L(T) versus on the temperature and $L_E(T)$ versus electric field for various values of temperature.

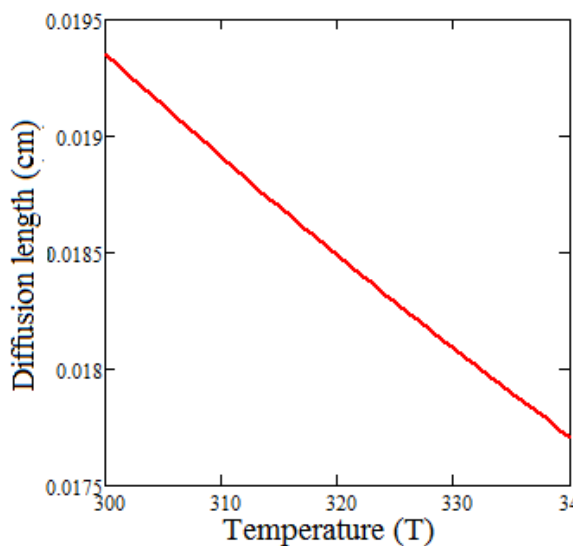


Figure 2a : Diffusion length at the absence of electrical polarization versus temperature

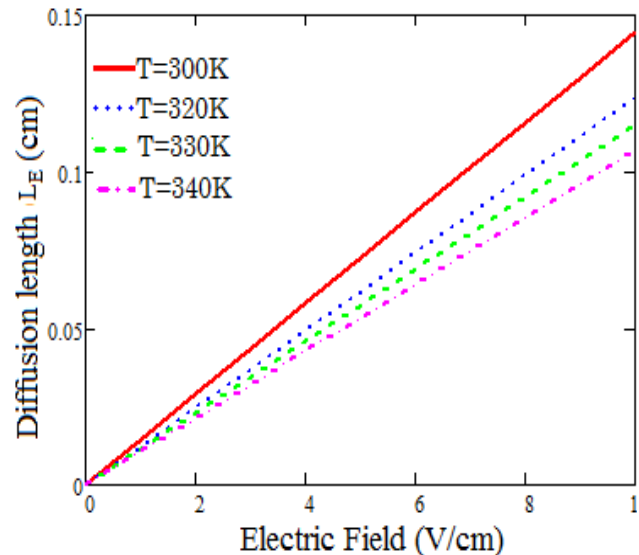


Figure 2b : Diffusion length of the minority charge carriers in the presence of an external electric field versus electric field



Figure 2a shows a decrease in diffusion length of the minority charge carriers no electric field with increasing temperature. Indeed, with increasing temperature, thermal agitation decreases the mobility of minority charge carriers and causes the decrease in the diffusion coefficient [13]. Thus, in view of equation 4 and the dependence of the diffusion length to the temperature, there is a decrease of the diffusion of the minority carriers when increasing temperature. In the presence of polarization (Figure 2b), we observe an increase of the diffusion length with the electric field intensity. Indeed, in the presence of electric field, the of minority charge carriers are accelerated toward the junction by the conduction phenomenon ($J_c = \mu (t) .E$) thus increasing the diffusion length of the minority charge carriers. We also observe that more the electric field is intense, more the diffusion length is temperature sensitive.

2.1.2. Study of the minority carrier’s density

We plot in figures 3a, b, c, d the minority carrier’s density versus base depth for different electric field values and for some of the temperature values T.

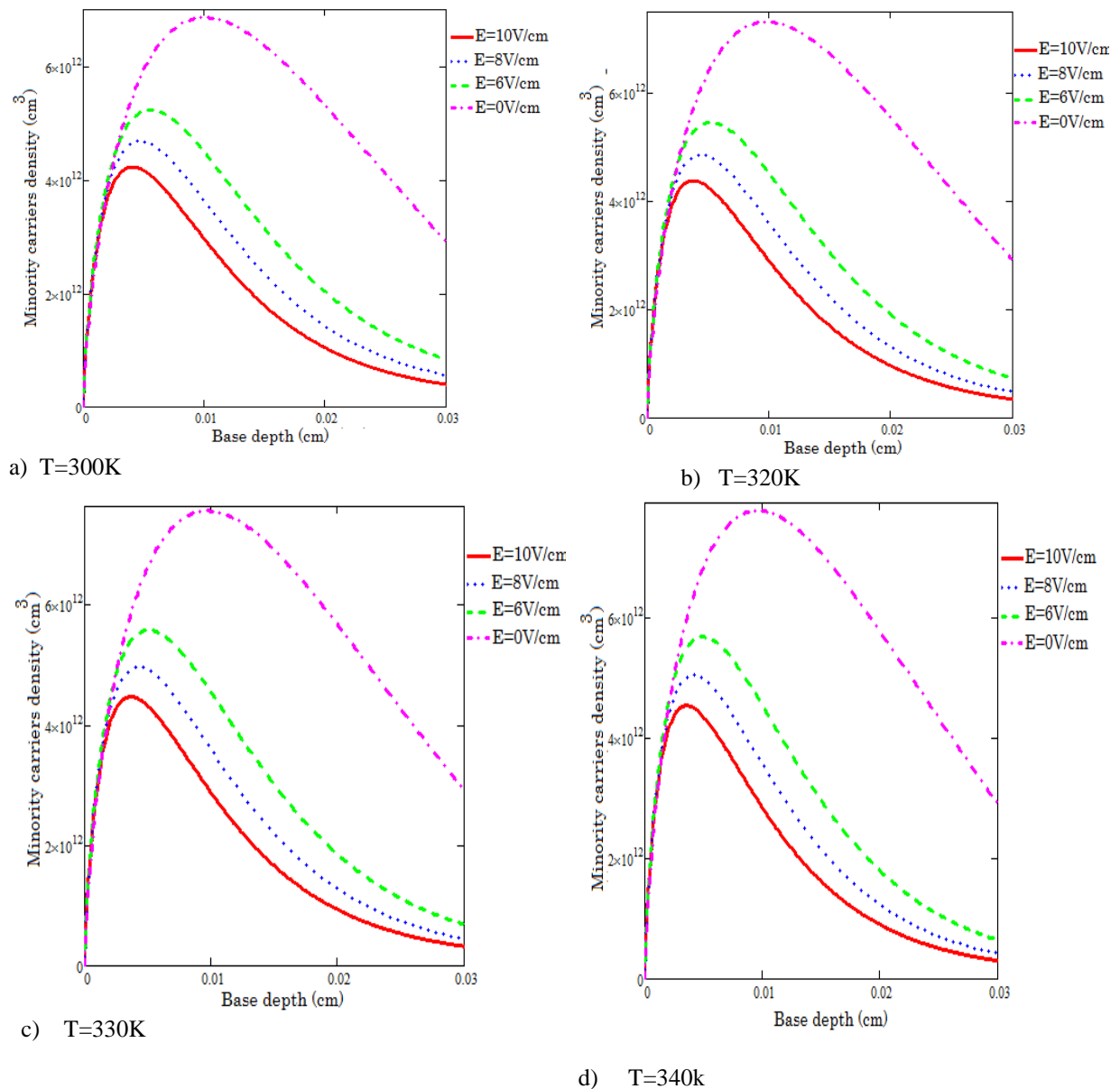


Figure 3: Minority carrier’s density versus base depth for different electric field values and for some of the temperature values T ($S_f=10^4$ cm/s, $S_b=10^3$ cm/s, $\tau=10^{-5}$ s)

We plot in figures 4a, b, c, d, e, f, g, h the minority carrier's density versus base depth for different of the temperature values T and for some electric field values.

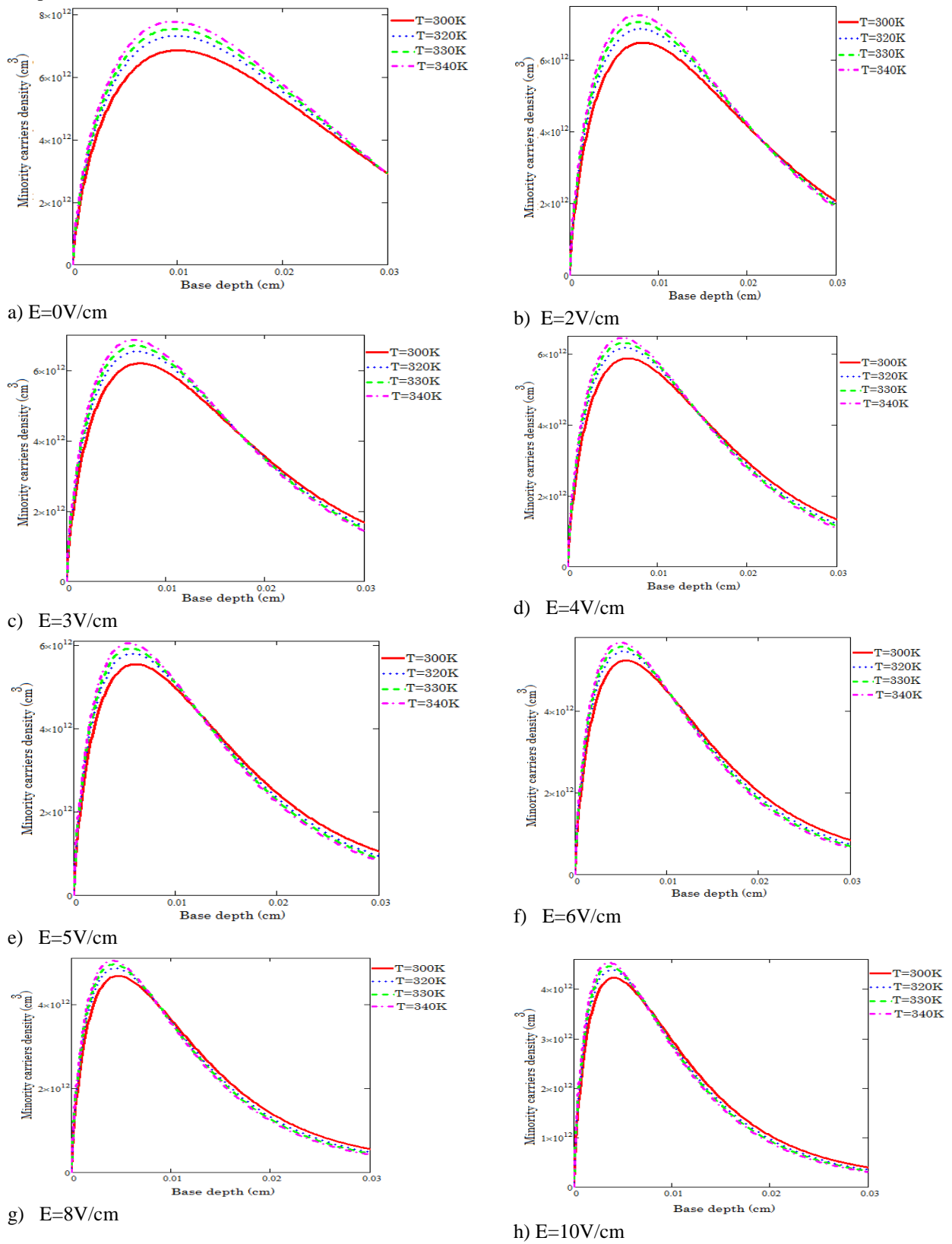


Figure 4: Minority carrier's density versus base depth for different temperature values and for some of the electric field values ($S_f=10^4\text{cm}^2/\text{s}$, $S_b=10^3\text{cm}^2/\text{s}$, $\tau=10^{-5}\text{s}$)

Figures 2 and 3 show that, for a given value of the electric field and temperature, the variation of the minority carrier density as a function of depth in the base has three essential observation areas. A first where the gradient is positive, the minority carriers located in this region are returned to the junction for participate in the production of the photocurrent. A second area, where the gradient is zero at a depth x_0 in the base, the minority carriers located in this region are blocked. A third zone where the gradient is negative, this region is characterized by a decrease the generation rate the minority carriers which is a exponential descending of the depth. we also notice an increase of the electric field is accompanied by a very significant reduction in the density of minority carriers near the junction (first zone) with for dual consequences : a decrease in the density of minority charge carriers and a displacement of the peaks of minority carriers density to the junction. The decrease of the minority carrier density peaks is caused by an increase of the minority carrier density which cross the junction for participates in the production of the photocurrent when the electric field increases. The displacement of these peaks to the junction shows an increase in the density of minority carriers to the junction when the electric field increases. The curves also show that the temperature increases the density of minority charge carriers and this increase is very important when the electric field increases.

2.2. Photocurrent density

The expression of the photocurrent density is deduced of currents diffusion and conduction ; we have :

$$J_{ph}(Sf, T, E) = q \cdot \left[D(T) \cdot \frac{\partial \delta(x, T, E)}{\partial x} \Big|_{x=0} + \mu(T) \cdot E \cdot \delta(0, T, E) \right] = q \cdot [Sf + \mu(T) \cdot E] \cdot \delta(0, T, E) \tag{11}$$

q is the charge of electron.

We plot in figures 5a, b, c, d , the photocurrent density versus junction recombination velocity for different electric field values and for some of the temperature values T .

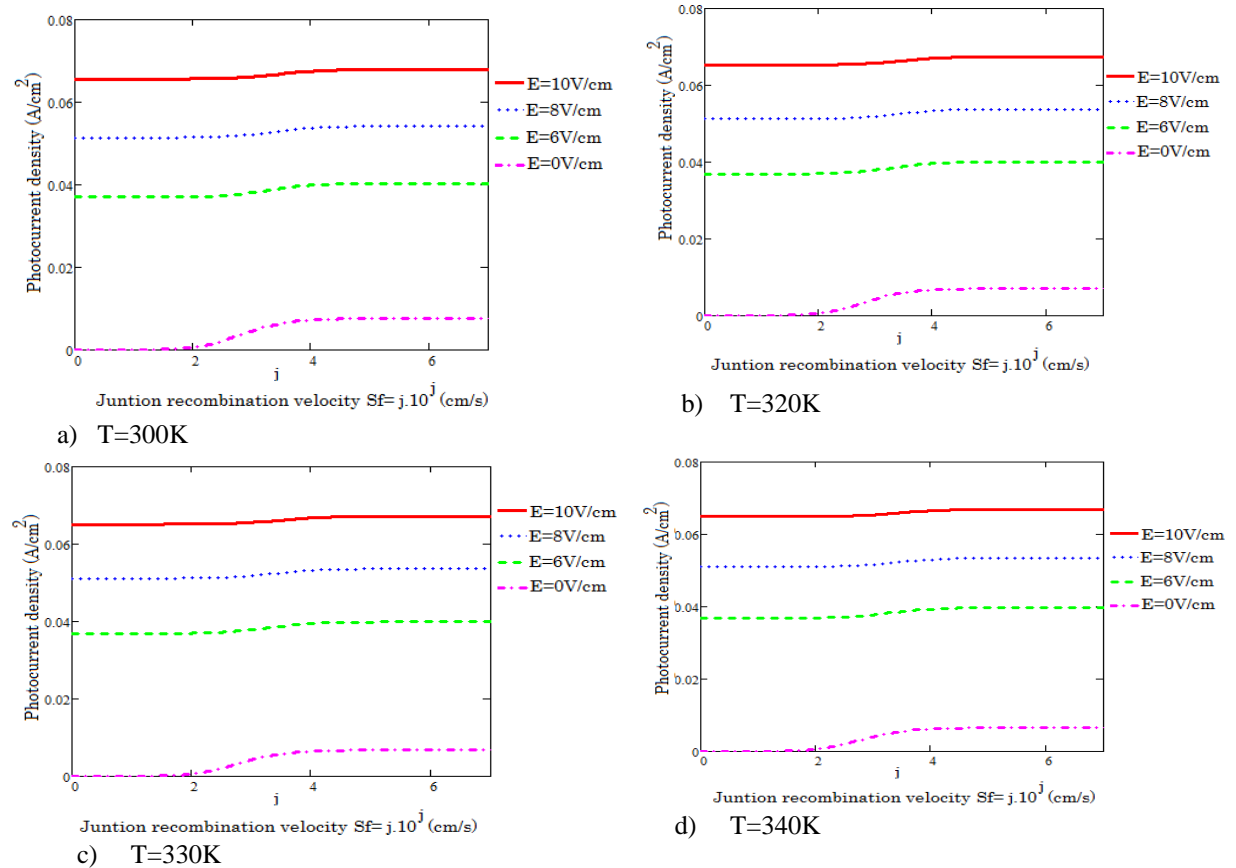


Figure 5: Photocurrent density versus junction recombination velocity for different electric field values and for some of the temperature values T ($\tau=10^{-5}$ s)

We plot in figures 6a, b, c, d, e, f, g, h the photocurrent density versus junction recombination velocity for different of the temperature values T and for some electric field values.

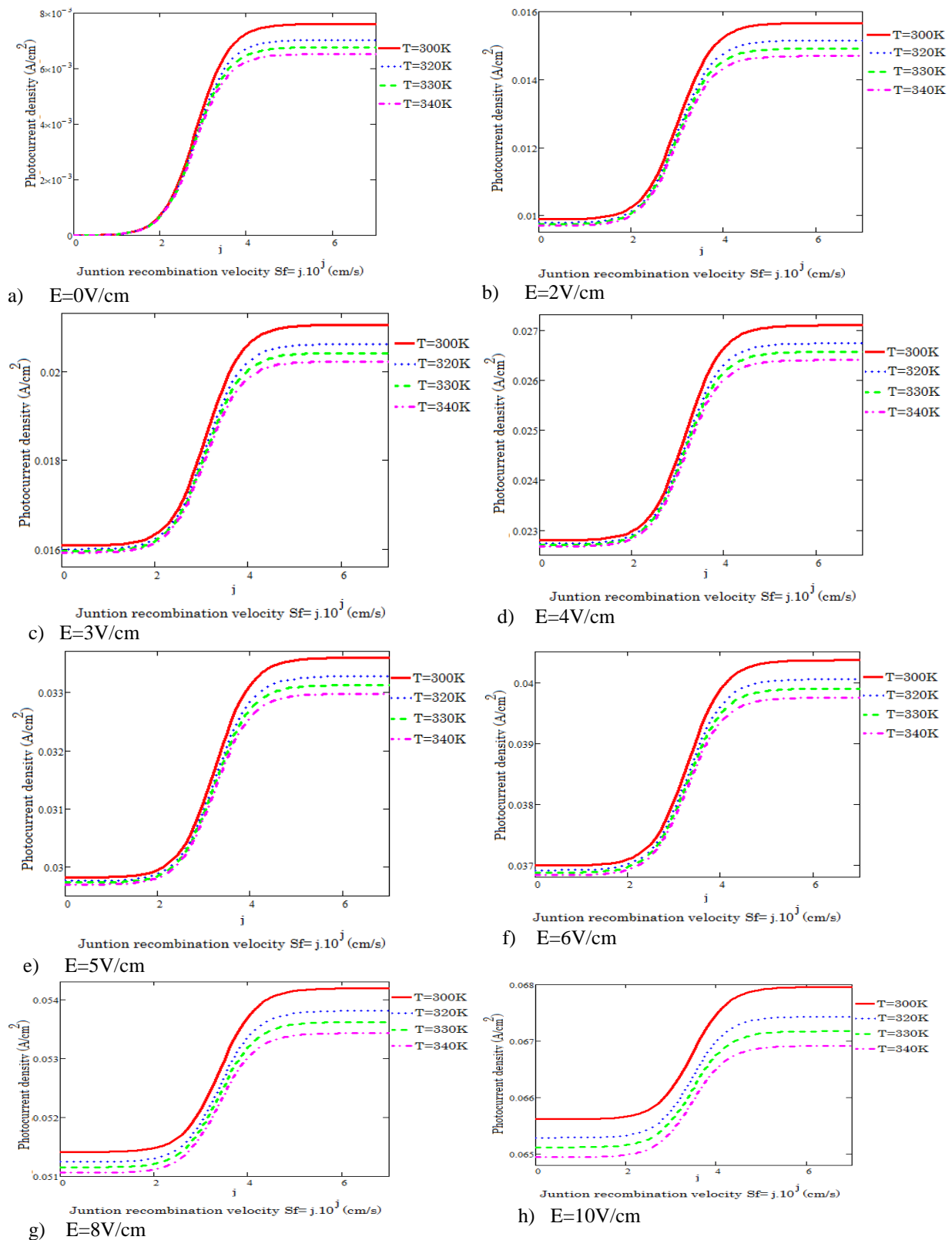


Figure 6: photocurrent density versus junction recombination velocity for different temperature values and for some electric field values ($\tau=10^{-5}$ s)

Figures 5 and 6 show two levels: a first at the vicinity of the open circuit (low Sf) and a second at the vicinity of the short circuit (large Sf). Near of the open circuit and at the lack of polarization (E = 0), the photocurrent is low. When Sf augment the flow of minority carriers at the junction increases and the photocurrent also increases up to a limit value (short-circuit current Jcc) where the photocurrent varies very little with Sf. This Sf limit value corresponds to the recombination velocity at the junction initiating the short circuit (sfcc) [19]. We are also seeing that a increase of the electric field causes in an increase of the photocurrent for all operating points of the solar cell. This result shows that the electric field, by conduction, increases the flow of carriers across the junction. We also observe a decrease in the photocurrent with increasing temperature and this decreasing becomes very important when the electric field increases.

2.3. Determination of the recombination velocity at the junction initiating a short-circuit condition.

The profile of the photocurrent density has showed a tray for high values of the recombination velocity at the junction. This value of the photocurrent density corresponds to the short-circuit current whose abscissa define the recombination velocity initiating the short circuit. We then obtain a short-circuit condition; from which following equation is deduced:

$$Jph(Sf, T, E) - Jcc(T, E) = 0 \tag{12}$$

The sort-circuit current (Jcc) is given by :

$$Jcc(T, E) = \lim_{Sf \rightarrow Sf_{cc}} Jph(Sf, T, E) \tag{13}$$

The recombination velocity at the junction initiating the short-circuit (Sfcc(T,E) is given by:

$$Sfcc(T, E) = \frac{\sum_{i=1}^3 [S_i + D(T) \cdot \phi(T) \cdot Sb(T, E) \cdot Ch(\phi(T) \cdot H)] [Y_1 + \mu(T) \cdot E \cdot X_1] - \beta(T) \cdot \phi(T) \cdot X_1 \cdot [D(T) \cdot \beta(T) \cdot V_1 - Z_1 \cdot D(T) \cdot b_i] - \mu(T) \cdot E \cdot X_1 \cdot [Y_1 + D(T) \cdot b_i \cdot U_1]}{-\beta(T) \cdot \phi(T) \cdot Z_1 \cdot X_1 + (\mu(T) \cdot E - b_i) U_1 + \mu(T) \cdot E \cdot U_1 \cdot X_1 - [Y_1 + (1 - b_i) X_1 + \mu(T) \cdot E X_1] U_1} \tag{14}$$

$$S_1 = [D^2(T) \cdot \phi^2(T) - (D(T) \cdot \beta(T) + Sb(T, E)) D(T) \cdot \beta(T)] Sh(\phi(T) \cdot H)$$

With :

$$S_1 = [D^2(T) \cdot \phi^2(T) - (D(T) \cdot \beta(T) + Sb(T, E)) D(T) \cdot \beta(T)] Sh(\phi(T) \cdot H) \tag{14-1}$$

$$U_1 = D(T) \cdot \phi(T) \cdot Ch(\phi(T) \cdot H) - (D(T) \cdot \beta(T) + Sb(T, E)) \cdot Sh(\phi(T) \cdot H) \tag{14-2}$$

$$V_1 = (D(T) \cdot b_i - Sb(T, E)) e^{-H(\beta(T) - D(T) \cdot b_i)} \tag{14-3}$$

$$X_1 = (D(T) \cdot \beta(T) + Sb(T, E)) \cdot Sh(\phi(T) \cdot H) + D(T) \cdot \phi(T) \cdot Ch(\phi(T) \cdot H) \tag{14-4}$$

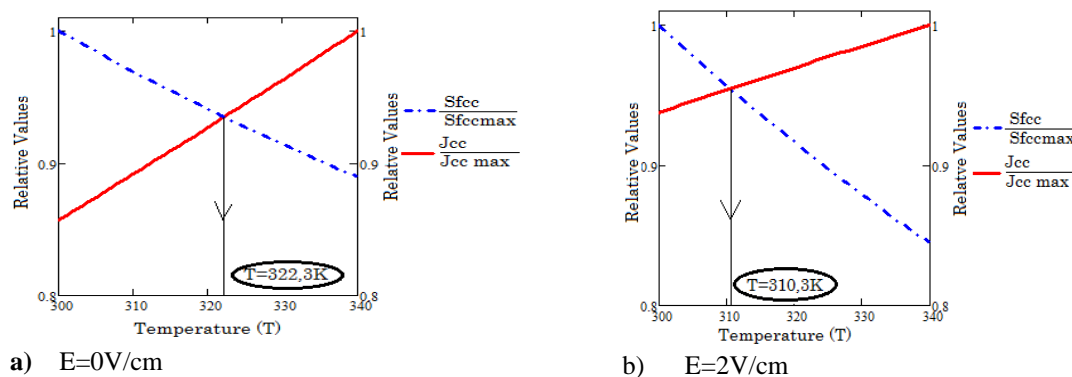
$$Y_1 = -\beta(T) \cdot \phi(T) \cdot (D(T) \cdot b_i - Sb(T, E)) e^{-H(\beta(T) - D(T) \cdot b_i)} - Z_1 \tag{14-5}$$

$$Z_1 = D(T) \cdot \phi(T) \cdot Sh(\phi(T) \cdot H) + (D(T) \cdot \beta(T) + Sb) Ch(\phi(T) \cdot H) \tag{14-6}$$

The back surface recombination Sb(T,E) can be expressed

$$Sb(T, E) = D(T) \cdot \frac{\sum_{i=1}^3 \phi(T) \cdot b_i \cdot (ch(\phi(T) \cdot H) - e^{-H(\beta(T)+b_i)}) - [\phi^2(T) - \beta(T) \cdot (b_i + \beta(T))] \cdot sh(\phi(T) \cdot H)}{\phi(T) \cdot (ch(\phi(T) \cdot H) - e^{-H(\beta(T)+b_i)}) - (b_i + \beta(T)) \cdot sh(\phi(T) \cdot H)} \tag{14-7}$$

We plot in Figures 7a, b, c, d, e, f, g, h the relative values of the recombination velocity at the junction initiating the short-circuit and the short-circuit current versus the temperature for different values of the electric field.



a) E=0V/cm

b) E=2V/cm



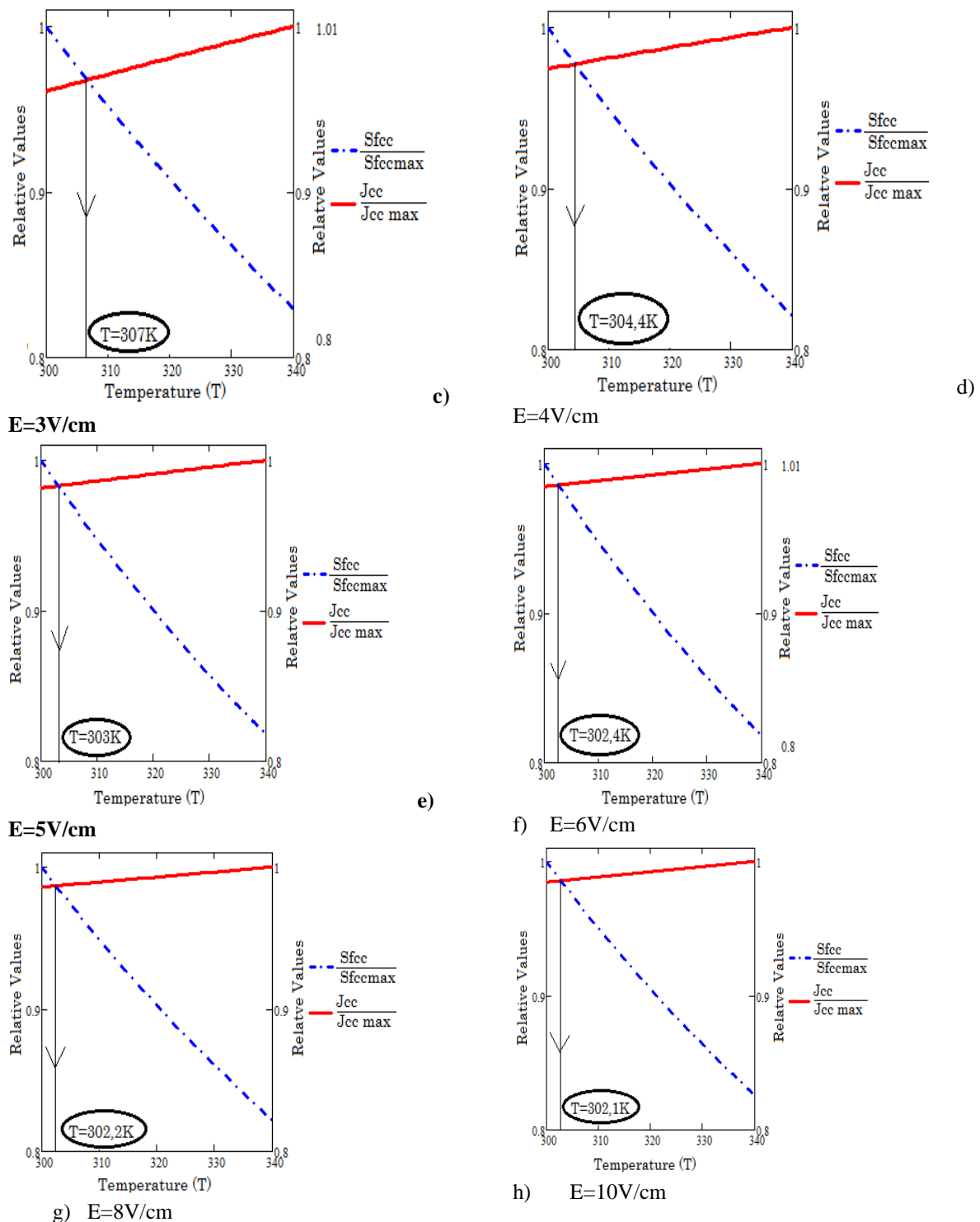


Figure 7: the relative values of recombination velocity at the junction initiating the short-circuit and the short-circuit versus the temperature for different values of electric champ.

The figure 6 show a decrease the relative values of the recombination velocity at the junction initiating the short-circuit and of the short-circuit current when the temperature increases. This decrease becomes very important when the electric field increases. We also observe a point of intersection for each figure and this point corresponds to a value of the temperature T: this value is the temperature at which the recombination velocity at the junction which initiates the short circuit [21] is obtained. This value of temperature decreases with the

increase of the electric field (see Figures 8a and b). Indeed, the short circuit condition is a solar cell operation point where the minority carriers density that cross the junction is maximum. The increase of the electric field allow, by conduction (in addition to the diffusion), increase of the density of minority carriers which cross the junction. This means that in presence of a electric field , the short-circuit situation can be achieved same for the low values of Sf.

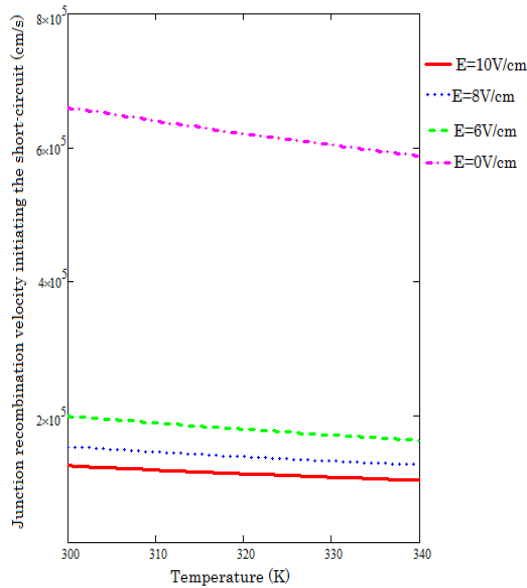


Figure 8a: Junction recombination velocity initiating the short-circuit versus temperature for different values of electric field

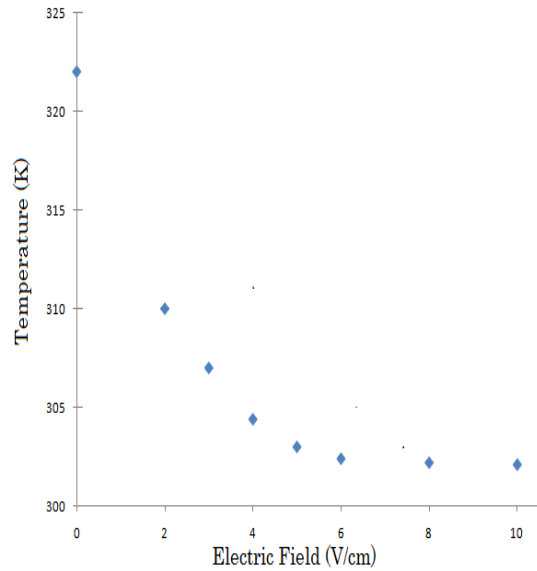


Figure 8b: Temperature versus electric field

3. Conclusion

In this study the expression of the charge minority carrier density is determined and its variation as a function of depth in the base for different electric field values is presented. The expression of the photocurrent is deduced from that of the charge minority carrier density and its change according to the recombination velocity at the junction for different values of electric field and for different temperature values is proposed. Thus, the recombination velocity at the junction initiating the short circuit is determined. The relative values of this velocity and those of the short-circuit current of current were studied in function of temperature for different values of the biasing electric field. This study showed that the external electrical bias augments the flow of charge minority carriers at the junction. Thus, when the electric field increases, the recombination velocity at the junction initiating the short circuit (sfcc) decreases. The study also showed that, the recombination velocity at the junction initiating the short- circuit decreases when the temperature increases. This decrease becomes important when electric field values are intense.

Références

- [1]. G. S. May, S. M. Sze. Fundamentals of Semiconductor Fabrication. First Edition, John Wiley & Sons, 2014.
- [2]. A. Goetzberger, J. Knobloch, B. Vob. Crystalline Silicon Solar Cell. John Wiley & Sons, 1998.
- [3]. B. Mazhari and H. Morkoç, Surface recombination in GaAs PN junction diode. J. App. Phys. 73(11), 1993, pp. 7509-7514
- [4]. H. El. Ghitani and S. Martinuzzi, Influence of dislocations on electrical properties of large grained polycrystalline silicon cells. J. App. Phys. 66(4), 1989, pp. 1717-1726
- [5]. R. Salach-Bielecki, T. Pisarkiewicz, T. Stapinski, P. Wojcik. Influence of junction parameters on the open circuit voltage decay in solar cells. Opto-Electronics Review 12 (1), 2004, pp.79-83



- [6]. E. Barsoukov et J. R. Macdonald. Impedance Spectroscopy: Theory, Experiment, and Applications. Second Edition, John Wiley & Sons, 2005.
- [7]. G. Sissoko, A. Corr ea, E. Nam ena, M. Adj, A. L. Ndiaye. Recombination parameters measurement in double sided surface field solar cell. World Renewable Energy Congress (1998), pp. 1856-1859.
- [8]. G. Sissoko, C. Museruka, A. Corr ea, I. Gaye, A. L. Ndiaye. Light spectral effect on recombination parameters of silicon solar cell. World Renewable Energy Congress (1996), part III, pp. 1487-1490.
- [9]. A. Dieng, I. Zerbo, M. Wade, A. S. Maiga, G. Sissoko. Three-dimensional study of a polycrystalline silicon solar cell: the influence of the applied magnetic field on the electrical parameters. *Semicond. Sci. Technol.* 26 (2011) 095023 (9pp).
- [10]. F. I. Barro, A. S. Maiga, A. Wereme, G. Sissoko. Determination of the recombination parameters in the base of a bifacial silicon solar cell under constant multispectral light. *Phys. Chem. News*, 56 (2010) pp.76-84.
- [11]. Agroui, K., 1999. Etude du comportement thermique de modules photovoltaïques de technologie monoverre et biverre au silicium cristallin. *Rev. Energ. Ren. Valorisation*, pp: 7-11.
- [12]. Le Quang Nam, M. Rodot, J. Nijs, M. Ghannam, and J. Copping. Réponse spectrale de photopiles de haut rendement au silicium multicristallin. *J. Phys. III (France 2, 1992)*, pp.1305-1316.
- [13]. M. Kunst and A. Sanders. Transport of excess carriers in silicon wafers. *Semicond. Sci. Technol.* 7, pp: 51-59 in the UK (1992).
- [14]. J. Furlan and S. Amon. Approximation of the carrier generation rate in illuminated silicon. *Solid State Electron*, 28 (1985), pp. 1241-43.
- [15]. S. N. Mohammad. An alternative method for the performance analysis of silicon solar cells. *J. Appl. Phys.* 61(2) 1987, pp. 767-777.
- [16]. D. L. Pulfrey. *Understanding Modern Transistors and Diodes*. Cambridge University Press, 2010.
- [17]. G. Sissoko, C. Museruka, A. Corr ea, I. Gaye and A. L. Ndiaye. Light spectral effect on recombination parameters of silicon solar cell. *Renewable Energy*. 3(1996), pp. 1487-1490.
- [18]. Sari-Ali, I., B. Benyoucef, B. Chikh-Bled, 2007. Etude de la jonction d'un semi-conducteur à l'équilibre thermodynamique. *J. Elect. Dev.* 5 : pp: 122-126.
- [19]. I. Ly, M. Ndiaye, M. Wade, Ndeye Thiam, Segala Gueye, G. Sissoko. Concept of Recombination Velocity S_{fc} At The Junction of A Bifacial Silicon Solar Cell, In Steady State, Initiating The Short-Circuit Condition. *Research Journal of Applied Sciences, Engineering and Technology* 5(1): 203-208, 2013.
- [20]. M. Zoungrana, B. Dieng, O.H. Lemrabott, F. Toure, M.A. Ould El Moujtaba, M.L. Sow and G. Sissoko. External Electric Field Influence on Charge Carriers and Electrical Parameters of Polycrystalline Silicon Solar Cell. *Research Journal of Applied Sciences, Engineering and Technology* 4(17); 2967-2972. 2012.
- [21]. Marcel Sitor Diouf, Gokhan Sahin, Amary Thiam, Khady Faye, Moussa Ibra Ngom, Doudou Gaye, Gr goire Sissoko. Determination of the junction surface recombination velocity limiting the open circuit (S_{fc}) for a bifacial silicon solar cell under external electric field. *International Journal of Innovative Science Engineering & Technology*, Vol. 2, Issue 9, September 2015, pp. 931- 938.

